Calculation of the energy barriers in strongly interacting many-particle systems

D. V. Berkov
INNOVENT e.V., Göschwitzer str. 22, D-07745, Jena, Germany

A numerical method which allows the evaluation of the energy barrier height between any two metastable states in a many-particle system with continuous degrees of freedom and arbitrary interparticle interaction is presented. The method uses the minimization of the Onsager–Machlup action corresponding to the given path between the two states. The path which minimizes this action is supposed to be the optimal path between the states under consideration and the height of the energy barrier separating these states is determined as the energy barrier along this optimal path. Test results for a simple two-dimensional potential (where the optimal path can easily be visualized) and for a dipolar glass are presented. © *1998 American Institute of Physics.* [S0021-8979(98)32611-0]

Evaluation of the energy (and free energy) barriers between metastable states in interacting many-particle systems is one of the most challenging problems in various areas of physics,[1] in particular, in the condensed matter physics of disordered systems with frustration like spin glasses.[2,3]

At the present time we lack general methods for the evaluation of these barrier heights, except, maybe, direct Monte Carlo simulations of the system escape over such barriers which are based on the Langevin equations[1,4,5] and can be applied only if the barrier height ΔE is comparable with the temperature T. In this contribution we would like to propose a numerical method which in its initial form is suitable for the energy barrier evaluation of arbitrary height in any *classical* interacting many particle system with continuous degrees of freedom, e.g., systems of ''usual'' classical particles, dipolar and RKKI spin glasses, Heisenberg (but not Ising!) models.

Main idea. Since the work of Onsager and Machlup,[6] it is well known (see also Ref. 7) that for a system of N classical particles which motion can be described by coordinates $\mathbf{x}=(x_1,\ldots,x_N)$ and velocities $\dot{\mathbf{x}}$ and which interaction energy $V(\mathbf{x})$ depends on their coordinates only the probability to observe a given trajectory $\mathbf{x}(t)$ for the transition between the two states A and B during the time t_f $[\mathbf{x}_A(0)\rightarrow\mathbf{x}_B(t_f)]$ is given by

$$P[\mathbf{x}(t)]\simeq J[\mathbf{x}]\exp\left[-\frac{S[\mathbf{x}(t)]}{4D}\right], \tag{1}$$

where the action $S[\mathbf{x}(t)]$ is defined as

$$S[\mathbf{x}(t),t_f]=\int_0^{t_f}dt\sum_i\left(\frac{dx_i}{dt}+\frac{\partial V(\mathbf{x})}{\partial x_i}\right)^2. \tag{2}$$

The form of the action (2) is the direct consequence of (i) the Langevin equations of the particle motion under the influence of the deterministic and random thermal forces (neglecting inertial terms) and (ii) the assumption that these thermal forces can be considered as independent Gaussian random quantities with zero correlation time. The Jacobian $J[\mathbf{x}]$ accounts for the variable transformation from the system coordinates to the thermal forces and the coefficient D in the exponent of (1) characterizes the thermal noise power and hence is proportional to the system temperature: $D\sim T$.

In principle, the statement (1) solves any problem related to the transition between A and B, because the total transition probability $P_{\text{tot}}(A\rightarrow B)$ is then given by the integral of (1) over all paths $\mathbf{x}(t)$ and transition times t_f. Unfortunately, the evaluation of the corresponding path integral is not possible for any interacting system of real interest, which is probably the reason why the idea outlined above was not used in real calculations except some oen-dimensional (1D) problems.[8,9]

However, it can be seen from (1) that in the low temperature limit ($D\rightarrow 0$ and hence $T\rightarrow 0$) the only significant contribution to $P[\mathbf{x}(t)]$ comes from the paths near the trajectory which minimizes the action $S[\mathbf{x}(t)]$; it is called an ''optimal'' path $\mathbf{x}_{\text{opt}}(t)$. In this case the energy barrier for the transition $A\rightarrow B$ can be found as the barrier along this trajectory: $\Delta E(A\rightarrow B)=E_{\max}(\mathbf{x}_{\text{opt}})-E_A$. So the ''only'' problem left is the minimization of the action functional $S(\mathbf{x})$.

The easiest way to perform this minimization is the approximation of the integral (2) by some numerical quadrature formula and the subsequent minimization of the many-variable function obtained this way. Approximating (2) by the simplest quadrature, we obtain

$$S_d(\mathbf{x})=\Delta t\sum_{i,k}\left[\frac{x_i^{k+1}-x_i^k}{\Delta t}+\frac{1}{2}\left(\frac{\partial V\{\mathbf{x}\}}{\partial x_i^{k+1}}+\frac{\partial V\{\mathbf{x}\}}{\partial x_i^k}\right)\right]^2, \tag{3}$$

where $\Delta t=t_f/K$, K is the number of time slices used, x_i^k is the coordinate of the ith particle at the time $t_k=k\Delta t$. The problem of the determination of the time slice number will be addressed elsewhere.[10] Minimization of $S_d(\mathbf{x})$ as a function of $N\cdot K$ variables x_i^k provides a discrete representation of the optimal path which can be used to calculate the corresponding energy barrier.

A simple test example. The result of the simplest possible test of the method, calculation of an optimal trajectory for a transition of a particle in a 2D space (x_1,x_2) between the two local minima of the potential

$$V(\mathbf{x})=\sum_j U_j\left[1+\left(\frac{\mathbf{x}-\mathbf{r}_j}{\Delta j}\right)^2\right]^{-1} \tag{4}$$

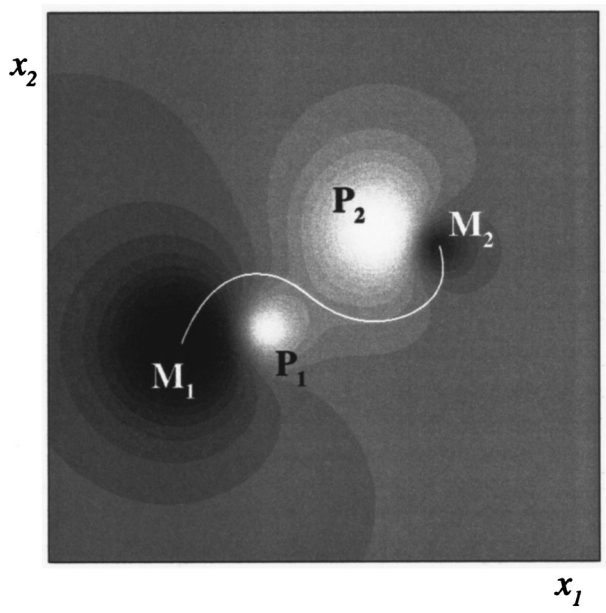

FIG. 1. Optimal trajectory (white line) for the particle transition between the two minima M_1 and M_2.

is shown in Fig. 1. The energy surface used possesses two peaks P_1 and P_2 ($U_j>0$) and two holes M_1 and M_2 ($U_j<0$). The starting trajectory for the minimization process was a straight line M_1-M_2. The final trajectory shown in Fig. 1 clearly passes through a saddle point providing the correct value of the energy barrier separating the minima M_1 and M_2 (a ''true'' optimal trajectory).

In this test case the optimal trajectory could be easily found due to a simple energy landscape. For a many-particle system, the search for a true optimal path between the two energy minima by the minimization of the action (2) [or (3)] is much more difficult, because this action has many local minima. Namely, any trajectory which proceeds along the gradient lines of the energy surface (i.e., for which $\dot{x}_i = \pm \partial V\{x\}/\partial x_i$) provides a local extremum to the action (2), see Ref. 9 for the proof in the 1D case.

For the energy surface presented in Fig. 1, this means, e.g., that the trajectory climbing along the gradient lines from M_1 up to P_1 and then going downhill from P_1 to M_2 also provides a local minimum to the action (2), and obviously gives a wrong value of the energy barrier (a ''false'' optimal trajectory). It is easy to construct an example where even the values of the action corresponding to the true and false optimal paths would be the same (just consider a system of two noninteracting particles each moving in a 1D double-well potential). For this reason, an additional analysis of the found optimal trajectories is necessary, so we developed an algorithm to distinguish between the true and false action minima (trajectories passing through the saddle points and climbing over the local maxima); due to the lack of space details of this algorithm will be described elsewhere.[10] Here we would like to present only its main idea: for many-particle systems with complicate energy landscape, we expect that *many different* local energy minima can be achieved when we minimize the system energy starting from any *energy maximum* and moving in different directions (in contrast to Fig. 1 where only two minima exist). For this reason, we have tried to find out which local energy minima can be found starting from various points scattered randomly in the vicinity of the trajectory point P_E with the largest energy. For a true optimal trajectory, P_E is a saddle point for the transition $M_1 \rightarrow M_2$ and the energy minimization starting P_E (or sufficiently close points) would bring us either to M_1 or to M_2. For a false optimal trajectory, P_E represents an energy maximum so that minimizing the system energy starting from P_E we would (with the probability rapidly growing with the particle number) discover other local minima different from both M_1 and M_2. This would indicate that P_E is a maximum rather than a saddle point and that the corresponding optimal trajectory is a false one.

Implementation of the method for a system of magnetic particles. Let us consider, e.g., a system of small identical single-domain ferromagnetic particles (fixed in a nonmagnetic matrix) each having the volume V and the saturation magnetization M_s and carrying the magnetic moment $\mathbf{m}_i$ of a constant magnitude $m_i = VM_s$. The magnetization state of such a system can be defined most conveniently using the spherical angles (θ_i, ϕ_i) characterizing the orientation of the ith magnetic moment. Below we denote the set of these spherical coordinates for all particles as Ω.

The action $S[\Omega(t)]$ corresponding to the transition $\Omega_A \rightarrow \Omega_B$ between the two given metastable states A and B of the system can be derived from the Landau–Lifshitz–Gilbert equations of motion for magnetic moments in the presence of thermal fluctuations[11] exactly as the action (2) is derived from the Langevin equations of motion for usual particles.[6,9] The result is (if the precession term can be neglected)

$$S[\Omega(t)] = \int_0^{t_f} dt \sum_i \left[\left(\frac{d\theta_i}{dt} + \frac{\partial E\{\Omega\}}{\partial \theta_i} \right)^2 + \left(\sin\theta_i \frac{d\phi_i}{dt} + \frac{1}{\sin\theta_i} \frac{\partial E\{\Omega\}}{\partial \phi_i} \right)^2 \right]. \quad (5)$$

Minimization of this functional in the Ω space gives the ''optimal'' path which can provide information about the energy barrier between the states Ω_A and Ω_B exactly as explained above.

The method was applied to a system of magnetic particles having the ''easy axis'' magnetic anisotropy with the energy $E_{\text{an}} = 0.5\beta M_s^2 V \sin^2\psi$, where $\beta(>0)$ is the reduced anisotropy constant and ψ is the angle between $\mathbf{m}$ and the easy axis direction $\mathbf{n}$. Without the external field (this was always the case for the results reported below) a single such particle has two equivalent equilibrium magnetization states (along the two opposite directions of the anisotropy axis) separated by the reduced energy barrier $\epsilon \equiv E/(M_s^2 V) = \beta/2$. The barrier found by our algorithm for a single such particle or for a system of noninteracting particles with different anisotropy constants agreed with this value within the numerical accuracy. The test on a *system* of noninteracting particles was necessary to ensure that the algorithm discriminating between the false and true local minima of the action works properly.

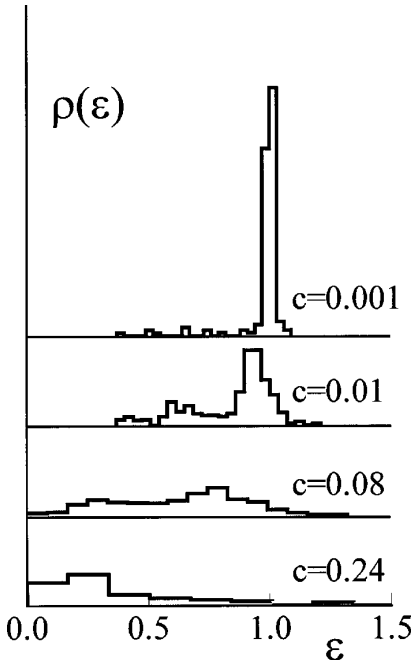

FIG. 2. Energy barrier distributions found by our algorithm for the system of $N=128$ dipolarly interacting magnetic particles with the uniaxial anisotropy ($\beta=2.0$) for various particle volume fractions c as shown in the figure.

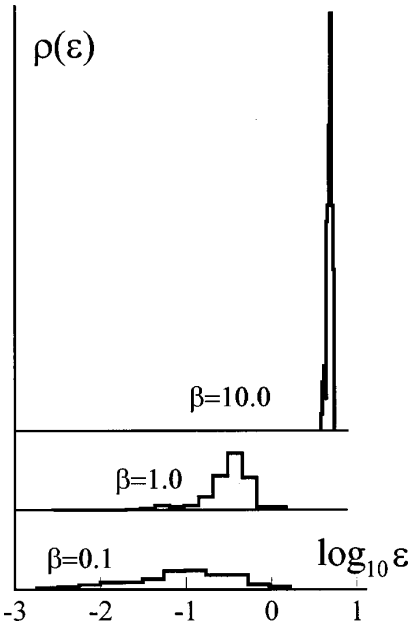

FIG. 3. The same as in Fig. 2 for systems of particles with the concentration $c=0.04$ and various anisotropy constants β as shown in the figure.

Next we considered a system of $N=128$ *dipolarly interacting* particles with equal anisotropies $\beta_0=2.0$ which were placed randomly (but nonoverlapping) in the cubic volume; periodic boundary conditions were assumed. The dependence of the energy barrier distribution on the particle volume concentration c was studied. To obtain the distribution density of energy barriers we have generated a number of (meta)stable states starting from various initial moment orientations and then minimized the actions (5) corresponding to the transitions between various pairs of these states. Typically for each histogram shown in Fig. 2 and Fig. 3 several hundred energy barriers were calculated.

Results of our simulations are shown in Fig. 2. As it should be, for the lowest concentration ($\eta=0.001$) almost all barriers are nearly equal to the single-particle barrier $\epsilon=\beta_0/2=1.0$ because for this concentration the interaction effects are almost negligible. Note, however, a few barriers well below this value which occur due to a strong interaction of particles positioned by chance very close to each other. Already for the next (still quite low) volume concentration $\eta=0.01$, a considerable amount of barriers with another (mostly lower) values occur, because a fraction of closely positioned particles increased. For the system with the moderate ($c=0.08$) and high ($c=0.24$) concentrations, the collective interaction effects lead to a qualitatively different energy barrier distribution strongly shifted to the lower energies.

Another example of such a transition from the single particle to the collective behaviour is presented in Fig. 3, where results of our simulations for a system of $N=128$ particles with the particle volume concentration $c=0.04$ and different single-particle anisotropy constants are shown (note the logarithmic scale of the energy axis). It can be seen that for the smallest anisotropy considered ($\beta=0.1$) collective effects clearly dominate, whereby all barriers found in the system with the largest anisotropy value ($\beta=10.0$) lie in the vicinity of the single-particle energy barrier $\epsilon=\beta/2=5.0$.

Due to the limited paper length we cannot discuss the relation between our results and experimental data, e.g., for magnetic viscosity[12,13] or ac susceptability of ferrofluids.[14] We only mention that care should be taken by establishing such a relation because (i) all experiments were performed at finite (and even not at *low*) temperatures so that the density of *free* energy barriers is required for their interpretation, (ii) transitions over different barriers lead to different moment changes which is essential for the calculation of both magnetic susceptibility and magnetic viscosity. Clearly further investigations are necessary.

[1] P. Hoenggi, P. Talkner, and M. Borkovec, Rev. Mod. Phys. **62**, 251 (1990).
[2] K. Binder and A. P. Young, Rev. Mod. Phys. **58**, 801 (1986).
[3] V. S. Dotsenko, Sov. Phys. Usp. (USA) **36**, 455 (1993).
[4] J. M. Gonzalez, R. Ramirez, R. Smirnov-Rueda, and J. Gonzalez, Phys. Rev. B **52**, 16034 (1995).
[5] J. M. Sancho, A. M. Lacasta, M. C. Torrent, J. Garcia-Ojalvo, and J. Tejada, Phys. Lett. A **181**, 335 (1993).
[6] L. Onsager and S. Machlup, Phys. Rev. **91**, 1505 (1953).
[7] R. Graham, in *Fluctuations, Instabilities and Phase Transitions*, edited by T. Riste (Plenum, New York, 1975).
[8] A. J. McKane, H. C. Luckock, and A. J. Bray, Phys. Rev. A **41**, 644 (1990).
[9] A. J. Bray and A. J. McKane, Phys. Rev. Lett. **62**, 493 (1989).
[10] D. V. Berkov, J. Magn. Magn. Mater. (accepted).
[11] W. F. Brown, Jr., Phys. Rev. **130**, 1677 (1963).
[12] X. Battle, M. Garcia del Muro, and A. Labarta, Phys. Rev. B **55**, 6440 (1997).
[13] D. Fiorani, A. M. Testa, E. Tronc, P. Prene, J. P. Joulivet, R. Cherkaoui, J. L. Dormann, and M. Nogues, J. Magn. Magn. Mater. **140–144**, 395 (1995).
[14] J. Zhang, C. Boyd, and W. Luo, Phys. Rev. Lett. **77**, 390 (1996).